

other. The angular dependence of the force couple (the rotation diagram) acting upon the bismuth monocystal was investigated at $T = 4.2^\circ \text{ K}$ for two constant values of the field.

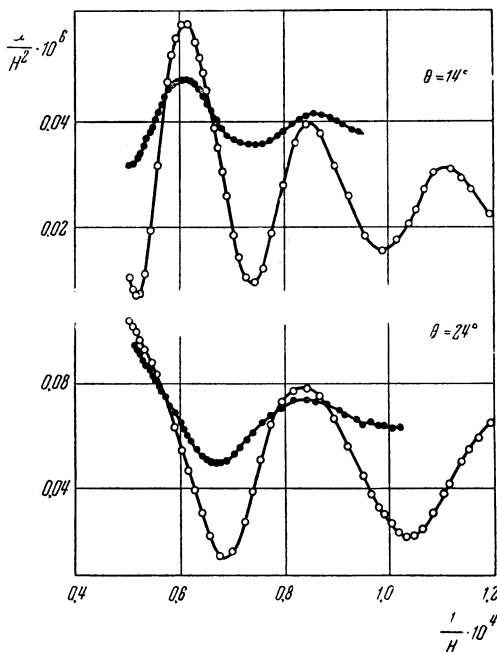


FIG. 2. Dependence of the difference between the components of the susceptibility of a bismuth monocystal upon the intensity of the applied magnetic field at $T = 4.2^\circ \text{ K}$; ●—under pressure $\sim 1500 \text{ kg/cm}^2$; ○—pressure removed.

Curves *a*, *c* and *e* of Fig. 1 represent the rotation diagrams for the bismuth monocystal determined in the absence of pressure; curve *b* is the rotation diagram for the same plane, but with a pressure $\sim 1500 \text{ kg/cm}^2$, while *d* is the rotation diagram for the same plane obtained upon removal and reapplication of a pressure on the order of 1500 kg/cm^2 . It is evident that uniform compression of the bismuth monocystal leads to a substantial reduction (by several times) in the amplitude of the oscillations. Removal of the pressure (curves *c* and *e* of Fig. 1) leads to almost complete restoration of the original form of the rotation diagram. The slight incompleteness of this restoration (actually a small pressure effect) is in all probability associated with deformation of the sample. It should be mentioned that a similar type of hysteresis is observed when the effect of pressure upon the galvanomagnetic properties of metals is investigated^{1,2}.

The dependence of the difference between the

two components of the susceptibility of the bismuth monocystal upon the field intensity was investigated for various values of θ . Two curves of this sort are presented in Fig. 2. It is evident that uniform compression of the bismuth monocystal leads to a substantial reduction in the amplitude of the oscillations with field strength, to an increase in the constant component of the susceptibility difference (the median line about which the oscillations take place), and also to a change in the period of the oscillations. Analysis of the curves showing the dependence of the difference in the components of the susceptibility upon the field strength for $\theta = \text{const}$ shows that for θ in the vicinity of 0 and 180° the period of the oscillations increases under pressure, while for θ near 90° it decreases. The change in the period of the oscillations of the susceptibility of bismuth monocystals under pressure on the order of 1500 kg/cm^2 is inconsiderable (it does not exceed a few percent).

¹ N. E. Alekseevskii and N. B. Brandt, J. Exptl. Theoret. Phys. (U.S.S.R.) **28**, 379 (1955); Soviet Phys. JETP **1**, 382 (1955).

² W. Overton and T. Berlincourt, Phys. Rev. **99**, 1165 (1955).

³ B. G. Lazarev and L. C. Kan, J. Exptl. Theoret. Phys. (U.S.S.R.) **14**, 470 (1944).

⁴ B. I. Verkin and I. F. Mikhailov, J. Exptl. Theoret. Phys. (U.S.S.R.) **25**, 471 (1953).

Translated by S. D. Elliott
114

On $K_{\mu 3}$ -Decay

S. G. MATINIAN

Academy of Science, Georgian SSR

(Submitted to JETP editor May 27, 1956)

J. Exptl. Theoret. Phys. (U.S.S.R.) **31**, 529-530

(September, 1956)

At the present time there have been definitely established five different decay schemes for K -mesons with masses $\sim 965 m_e$. The decay products are known for three of these ($K_{\pi 2}$, $K_{\mu 2}$, $K_{\pi 3}$).

It has recently been established^{1,2} that one of

the neutral particles emerging from the $K_{\mu 3}$ decay should be a π^0 -meson, and that the mass of the other particle is zero. On the other hand, a half-integral spin for the K -meson leads to difficulties when one examines the process of K -meson formation in nuclear collisions^{1,3}.

The most probable decay scheme appears to be:

$$K_{\mu 3} \rightarrow \mu + \pi^0 + \nu. \quad (1)$$

The purpose of this note is to calculate the energy spectrum of the μ -mesons and π^0 -mesons in the $K_{\mu 3}$ -decay and to estimate the decay constant.

Regarding the $K_{\mu 3}$ as a scalar (or pseudoscalar) particle and limiting consideration to the direct coupling of fields, one obtains for the interaction Hamiltonian density:

$$H' = g (\bar{\Psi}_\mu \gamma \psi_\nu) (\varphi_\pi^+ \varphi_K), \quad (2)$$

where $\gamma = \gamma_5$ or 1, respectively, for scalar or pseudoscalar particles, and g is a constant with the dimensions of a length.

For finding the energy spectrum of the μ - and π^0 -mesons, the method of Ref. 4 is convenient. The results are the same for both scalar and pseudoscalar $K_{\mu 3}$ -mesons, due to the vanishing rest mass of the neutrino.

The energy spectrum of the μ -mesons:

$$w dE_\mu = \frac{g^2}{32\pi^3} \frac{(A - 2ME_\mu) \sqrt{E_\pi^2 - m_\pi^2}}{M(B - 2ME_\mu)^2} \quad (3)$$

$$\times \{C + DE_\mu - 2M^2 E_\mu^2\} dE_\mu$$

The energy spectrum of the π^0 -mesons:

$$w dE_\pi = \frac{g^2}{32\pi^3} \frac{(G - 2ME_\pi)^2}{M(F - 2ME_\pi)} \sqrt{E_\pi^2 - m_\pi^2} dE_\pi; \quad (4)$$

E and E_π are the total energies of the μ - and π^0 -mesons in the rest system of the $K_{\mu 3}$ -meson ($\hbar = c = 1$);

$$\begin{aligned} A &= M^2 + m_\mu^2 - m_\pi^2; & B &= M^2 + m_\mu^2; & (5) \\ C &= m_\mu^2 (m_\pi^2 - m_\mu^2 - M^2); \\ D &= M (M^2 + 3m_\mu^2 - m_\pi^2); \\ F &= M^2 + m_\pi^2; & G &= M^2 + m_\pi^2 - m_\mu^2 \end{aligned}$$

Integrating (4) from m_π to $(M^2 + m_\pi^2 - m_\mu^2) / 2M$ we obtain for the total probability of decay

$$w_{\mu 3} = (gm_\pi)^2 (32\pi^3)^{-1} 0.95 \cdot 10^{23} \text{ sec}^{-1}. \quad (6)$$

From this, using $\tau \approx 10^{-8}$ sec, we find

$$(g^2 / 4\pi) m_\pi^2 \approx 10^{-13}. \quad (7)$$

The correctness of the scheme corresponding to Eq. (1) for $K_{e 3}$ -decay is not yet established with sufficient certainty¹. A similar calculation for the scheme

$$K_{e 3} \rightarrow e + \nu + \pi^0 \quad (8)$$

gives

$$w_{e 3} = (g'm_\pi)^2 (32\pi^3)^{-1} \cdot 6,42 \cdot 10^{23} \text{ sec}^{-1} \quad (9)$$

where g' is the corresponding coupling constant for the four fields. Comparing (6) and (9) we obtain

$$w_{\mu 3} / w_{e 3} \approx 0,16 (g / g')^2. \quad (10)$$

From the results of Ref. 5, it follows that $w_{\mu 3} / w_{e 3} \approx 0.5$. Then we have $g' = 0.6 g$. However, it is necessary to note that the present statistics are inadequate for an unambiguous answer to the question of the ratio of $w_{\mu 3}$ and $w_{e 3}$, and consequently of the equality of the constants g and g' .

In conclusion, we remark that the $K_{\mu 3}$ -decay scheme can be connected with the $K_{\mu 2}$ -decay in the following way*:

$$K_{\mu 3} \xrightarrow{\eta} (K_{\mu 2}) + \pi^0 \xrightarrow{f} \mu + \nu + \pi^0, \quad (11)$$

where η is the strong interaction constant (those interactions which do not violate "strangeness"), and f is the weak interaction constant (e.g., the universal weak Boson-Fermion interaction⁷).

Finally, the author considers it his pleasant duty to express his gratitude to G. R. Khutsishvili for constant help during the course of this work.

* In Ref. 6, the $K_{\mu 3}$ -scheme was connected with the scheme $K_{\pi 2} (K_{\mu 3} \rightarrow K_{\pi 2} \rightarrow \pi + \pi^0 \rightarrow \mu + \nu + \pi^0)$, but led to the result $w_{K_{\mu 3}} / w_{K_{\pi 2}} \approx 10^{-14}$, in contradiction to experiment.

¹ Kaplon, Klarman and Yekutieli, Phys. Rev. **99**, 1528 (1955).

² Huang, Kaplon and Yekutieli, Bull. Am. Phys. Soc. **1**, 64 (1956).

³ A. Pais and R. Serber, Phys. Rev. **99**, 1551 (1955).

⁴ O. Kofoed-Hansen, Phil. Mag. **42**, 1411 (1951).

⁵ J. Grussard, *et al.*, Nuovo Cimento **3**, 731 (1956).

⁶ G. Gosta and N. Dellaporta, Nuovo Cimento **2**, 519 (1955).

⁷ K. Iwata, *et al.*, Progr. Theor. Phys. **13**, 19 (1955).

Translated by C. R. Lubitz

107

Measurement of the Lifetimes of *K*-Mesons

M.IA. BALATS, P.I. LEBEDEV AND I.U.V. OBUKHOV

(Submitted to JETP editor June 7, 1956)

J. Exptl. Theoret. Phys. (U.S.S.R.) **31**, 531-533

(September, 1956)

THE measurement of the mean life of charged *K*-mesons from cosmic radiation has been carried out at sea level, using scintillation counters and a high-speed oscillograph¹. A charged unstable particle formed in a slab of lead *A* (Fig. 1) passed through counters *C*₁ and *C*₂, and reached counter *C*₁ inside which was a brass absorber (10 gm/cm²). Counters *C*₃ and *C*₃' then registered the decay

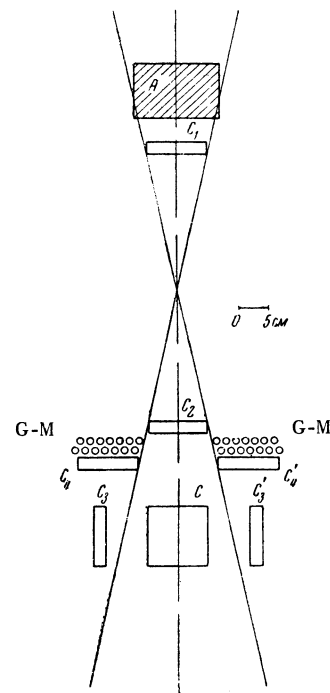


FIG. 1. Schematic diagram of set-up.

products of the particles which came to rest in *C*. The data on the liquid scintillation counters are collected below in a Table.

TABLE

Counter	Area cm ²	Thickness, cm	Solvent	Conc. of Terphenyl, g/l	Amount of FEU-19
<i>C</i> ₁ , <i>C</i> ₂ , <i>C</i> ₃ , <i>C</i> ₃ '	10×20	2	Toulene	3.5	1
<i>C</i> ₄ , <i>C</i> ₄ '	10×26	2	Benzene	1.4	2
<i>C</i>	10×20	10	Benzene	0.9	1

Pulses from the photomultipliers of the counters *C*₁, *C*₂, *C*₃ and *C*₃' were amplified, time-formed and fed to a coincidence counter². The amplifier band width was 210 mc, the amplification factor ~6. In channels *C*₁ and *C*₂ pulses of length 4×10^{-8} sec were formed, in channels *C*₃ and *C*₃', of length 6×10^{-9} sec. The resolution curve of the coincidence circuit is given in Fig. 2. Triple coincidences *C*₁ + *C*₂ + *C*₃ or *C*₁ + *C*₂ + *C*₃' triggered the oscilloscope and pulses coming from counter *C* were fed to the input of the vertical deflection amplifier. They were then photographed

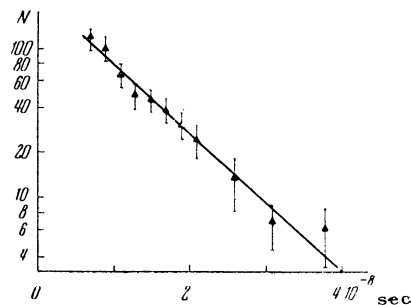


FIG. 2. Resolution curve for triple coincidences *C*₁ + *C*₂ + *C*₃.